Arabian Journal of Chemistry (2013) 6, 413–422

King Saud University

Arabian Journal of Chemistry

www.ksu.edu.sa
www.sciencedirect.com

ORIGINAL ARTICLE

Inhibition effect of hexadecyl pyridinium bromide on the corrosion behavior of some austenitic stainless steels in H_2SO_4 solutions

M.M. Hamza [a], S.S. Abd El Rehim [a], Magdy A.M. Ibrahim [a,b,*]

[a] *Chemistry Department, Faculty of Science, Ain Shams University, Cairo 11566, Egypt*
[b] *Chemistry Department, Faculty of Science, Taibah University, Al Madina Al Mounwara 30002, Saudi Arabia*

This paper is dedicated to the memory of Dr. M.M. Hamza (1962-2009).

Received 17 October 2010; accepted 9 November 2010
Available online 9 December 2010

KEYWORDS

Hexadecyl pyridinium bromide;
Corrosion;
Impedance spectroscopy;
Stainless steel;
Inhibitors

Abstract The inhibition effect of hexadecyl pyridinium bromide (HDPB) as a cationic surfactant on the corrosion behavior of some Egyptian austenitic stainless steel SS 304L, SS 316H and SS 304H in 0.5 M H_2SO_4 solutions was investigated by using potentiodynamic polarization technique and electrochemical impedance spectroscopy (EIS). The results indicate that HDPB is a good inhibitor for the samples under investigation in 0.5 M H_2SO_4 solutions. In addition, the inhibition efficiency $\eta\%$ increases with the inhibitor concentration while decreases with the increasing temperature referring to physical adsorption. The adsorption of the inhibitor obeys a Temkin adsorption isotherm. Polarization curves show that HDPB is a mixed inhibitor in H_2SO_4 solutions. The results obtained from polarization and impedance measurements are in good agreement. Activation-free energies, enthalpies, and entropies for the inhibition process of HDPB were determined.

1. Introduction

Due to its wide applications in industry, the electrochemical properties of austenitic stainless steel are the subject of many studies (Abd El Rehim et al., 1985; Ibrahim et al., 2002, 2008; Yang and Luo, 2001; Rybalka et al., 2006; Ameer et al., 2004).

During industrial-cleaning processes, such as: acid descaling, acid pickling, oil-well acid in oil recovery process, and in petrochemical processes, the use of sulfuric acid and hydrochloric acid leads to destructive effects on the metal surface. Therefore, inhibition of corrosion is clearly very essential. Surfactants represent an important category of organic

* Corresponding author at: Chemistry Department, Faculty of Science, Taibah University, Al Madina Al Mounwara 30002, Saudi Arabia. Tel.: +966 501221667; fax: +966 48470235.
E-mail address: imagdy1963@hotmail.com (M.A.M. Ibrahim).

Peer review under responsibility of King Saud University.
doi:10.1016/j.arabjc.2010.11.002

Production and hosting by Elsevier

compounds, which are used widely in industry especially in electrodeposition of metals (Ibrahim, 2000a,b; Ibrahim et al., 2004, 2006) and as corrosion inhibitors for metals in different acidic solutions (Abd El Rehim et al., 2008; Tavakoli et al., 2008; Saleh, 2006; Abd El Maksoud, 2004). The inhibition properties of the surfactants are frequently defined at a specific concentration of the surfactant called "the critical micelle concentration" CMC. At the CMC, a surfactant is capable of forming micelles (ordered structures), which exist together with isolated molecules in solution in an equilibrium controlled by hydrophobic interaction between surfactant hydrocarbons' tails and the solvent, together with attractive hydration and repulsive electrostatic forces on the hydrophilic heads.

In sulfuric acid solution, cationic surfactant has a lower extent of adsorption due to low adsorbability of the SO_4^{2-} ions (Frignani et al., 1983; Bentiss et al., 2001). However, in the presence of halide ion either as a counter ion or in solution, it helps to increase the extent of adsorption due to the well-known synergistic effects (Schweinsberg and Ashworth, 1988; Popova et al., 2003). The presence of π-bonding electrons via aromatic ring in the molecular structure of the cationic surfactant has a great influence on the mode and the extent of adsorption of the cationic surfactant on metal surface.

The objective of the present work was to study the applicability of HDPB, cationic surfactant, as a corrosion inhibitor for SS 304L, SS 316H and SS 304H samples in sulfuric acid solutions. It is also aimed to predict the thermodynamic feasibility of adsorption of the inhibitor molecule on SS surface and to study its adsorption behavior.

2. Experimental

The austenitic stainless steel samples used in the present work were produced in the induction furnace of the Modern Foundries Company, Giza, Egypt. The working electrode was in the form of rod (5 mm diameter) and was enclosed in a Pyrex glass tube sealed with Araldite to offer an exposed surface area of 0.28 cm^2. The chemical composition of these alloys is given in Table 1.

The electrode was abraded with a series of emery papers, from a coarse grade 500 and proceeding in steps to fine grade 1500, washed thoroughly with doubly distilled water, and then introduced into the test solution. A platinum wire was used as a counter electrode. All potentials were measured against a saturated calomel electrode. The measurements were carried out in three-electrode cell by using a computer-assisted Potentiostat ACM. The cell was placed in a water thermostat to attain the required temperature ±1.0 °C. All solutions were freshly prepared from analytical grade chemicals and doubly distilled water. The aqueous corrosion behavior of the alloys was studied by using potentiodynamic polarization technique and the electrochemical impedance spectroscopy (EIS). The potentiodynamic polarization (E/j) curves were recorded by sweeping the potential from the starting potential towards more positive direction (from about −700 mV to about −250 mV) with a scan rate of 20 mV s^{-1}. EIS measurements were carried out in a frequency range of 30 kHz to 1 Hz using an amplitude of 10 mV peak to peak using AC signal at the open circuit potential. Duplicate experiments were carried out to ensure reproducibility. The numerical values R_{ct} and C_{dl} for the present systems were determined by an analysis of Nyquist and Bode plots and the equivalent circuit was determined by means of a computer program ACM Instrument-Gill AC automated potentiostat ZRA EIS/AC Impedance Galvanostats and LPR meters. The hexadecyl pyridinium bromide, HDPB ($C_{21}H_{38}BrN{\cdot}H_2O$) has the following structure:

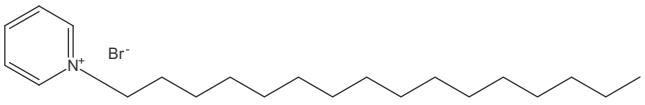

3. Results and discussion

3.1. Potentiodynamic polarization measurements

Figs. 1–3 show the potentiodynamic cathodic and anodic polarization curves for SS 304L, SS 316H and SS 304H samples in 0.50 M H_2SO_4 solution in the absence and presence of various concentrations of HDPB (10^{-6} to 3×10^{-2} M) at 25 °C. The curves were swept starting from negative potential and going to the positive direction with a scan rate of 20 mV s^{-1}. The electrochemical parameters, corrosion potential, E_{corr} and corrosion current j_{corr} derived from these curves were obtained and listed in Table 2.

Fig. 1 shows the potentiodynamic polarization curves for SS 304L sample in 0.50 M H_2SO_4 solution. It is clear that the addition of low concentrations of HDPB (10^{-6}–10^{-4} M) to the acid solution decreases the hydrogen evolution potential, but has no significant influence on the dissolution potential. However, high concentrations of HDPB enhance both the cathodic and anodic potentials. Data of Table 2 show that the presence of these low concentrations of HDPB in the solution increases the value of j_{corr} indicating acceleration of corrosion. The acceleration effect of this surfactant decreases with increasing its concentration. Acceleration of corrosion in the presence of low concentrations of surface-active compounds with long chain alkyl group in H_2SO_4 solutions has been reported previously (Larabi et al., 2004; Podobaev and Stolyarov, 1971). The acceleration may be due to the decrease in the potential of cathodic hydrogen evolution. It may also be due to the adsorption of impurity particles on the alloy surface, which reduces the metal binding energy and thus affects the magnitude and mechanism of hydrogen overpotential

Table 1 Chemical composition (wt.%) of the austenitic stainless steel alloys.

	C	Si	Mn	Cr	Ni	Mo	P	S	Cu
SS 304L	0.033	0.330	1.900	18.01	8.11	0.09	0.031	0.004	2.180
SS 316H	0.200	1.130	1.250	18.35	8.80	2.00	0.028	0.008	0.240
SS 304H	0.220	1.250	1.200	19.45	9.45	1.15	0.025	0.015	0.200

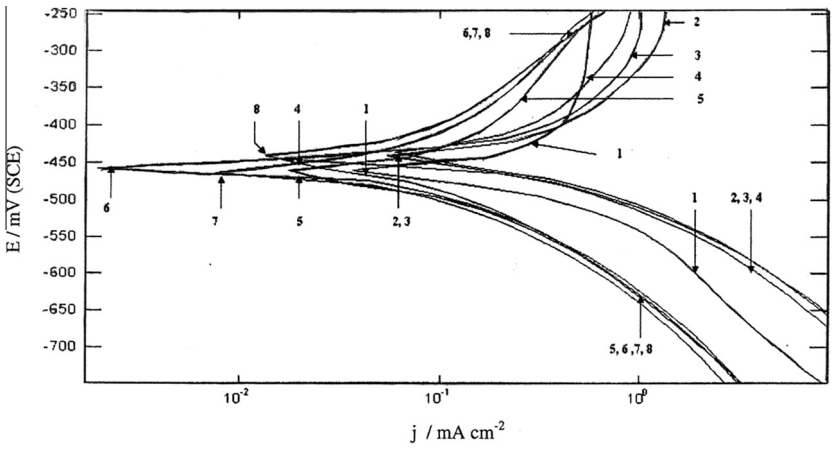

Figure 1 Cathodic and anodic potentiodynamic polarization curves of SS 304L alloy in 0.50 M H_2SO_4 solution in the absence and presence of various concentrations of HDPB at a scan rate of 20 mV s^{-1} and at 25 °C. (1) Blank; (2) 10^{-6} M; (3) 10^{-5} M; (4) 10^{-4} M; (5) 10^{-2} M; (6) 0.02 M; (7) 0.03 M; (8) 0.04 M HDPB.

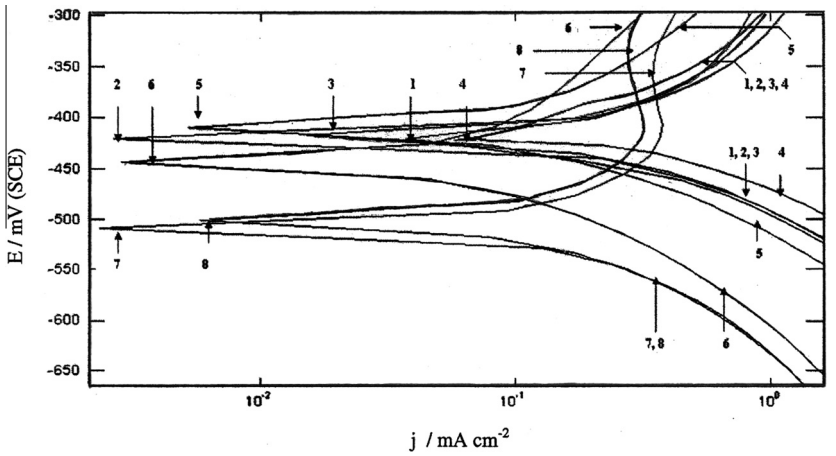

Figure 2 Cathodic and anodic potentiodynamic polarization curves of SS 316H alloy in 0.50 M H_2SO_4 solution in the absence and presence of various concentrations of HDPB at a scan rate of 20 mV s^{-1} and at 25 °C. (1) Blank; (2) 10^{-6} M; (3) 10^{-5} M; (4) 10^{-4} M; (5) 10^{-3} M; (6) 10^{-2} M; (7) 0.02 M; (8) 0.03 M HDPB.

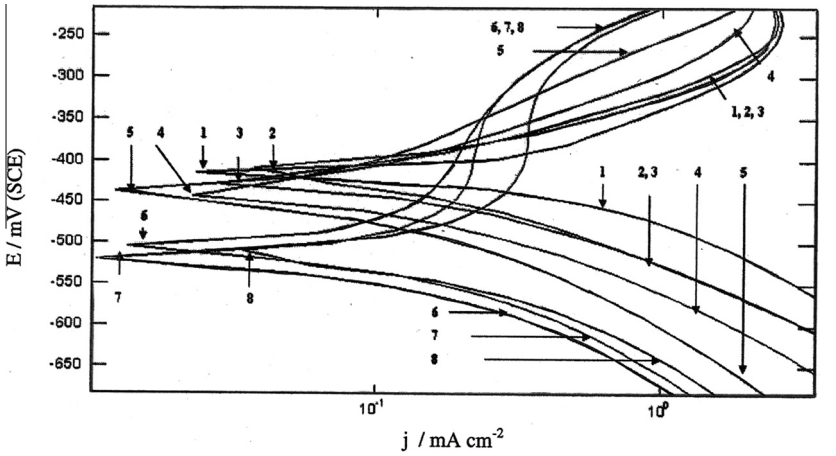

Figure 3 Cathodic and anodic potentiodynamic polarization curves of SS 304H alloy in 0.50 M H_2SO_4 solution in the absence and presence of various concentrations of HDPB at a scan rate of 20 mV s^{-1} and at 25 °C. (1) Blank; (2) 10^{-6} M; (3) 10^{-5} M; (4) 10^{-4} M; (5) 10^{-3} M; (6) 10^{-2} M; (7) 0.02 M; (8) 0.03 M HDPB.

Table 2 Electrochemical parameters, E_{corr}, j_{corr} and $\eta\%$ associated with polarization measurements recorded for SS 304L, SS 316L and SS 304H in 0.50 M H_2SO_4 solution in the absence and presence of various concentrations of HDPB at 25 °C.

Concentration (M)	SS 304L			Concentration (M)	SS 316 H			Concentration (M)	SS 304H		
	$-E_{corr}$ (mV)	j_{corr} (mA cm^{-2})	$\eta\%$		$-E_{corr}$ (mV)	j_{corr} (mA cm^{-2})	$\eta\%$		$-E_{corr}$ (mV)	j_{corr} (mA cm^{-2})	$\eta\%$
0.0	460	22.3		0.0	427	65.4		0.0	420	53.5	
10^{-6}	460	26.5		10^{-6}	425	49.5	23.6	10^{-6}	410	27.1	49.5
10^{-5}	465	23.8		10^{-5}	417	29.6	54.3	10^{-5}	430	21.9	59.2
10^{-4}	465	22.9		10^{-4}	413	29.9	54.7	10^{-4}	445	20.8	61.1
10^{-2}	465	13.0	41.9	10^{-3}	410	28.7	56.1	10^{-3}	438	14.5	72.9
0.02	462	7.1	68.1	10^{-2}	445	11.0	83.2	10^{-2}	505	8.2	84.8
0.03	470	6.4	71.2	0.02	510	5.8	91.1	0.02	520	5.8	89.3
0.04	445	4.9	77.7	0.03	502	5.8	91.1	0.03	510	5.9	88.9

(Riggs, 1973). However, concentrations of HDPB higher than 10^{-3} M decrease the value of j_{corr}, for SS 304L indicating corrosion inhibition. In the case of SS 316H and SS 304H (Figs. 2 and 3), it was found that at all concentration ranges studied, even the smallest one, HDPB causes inhibition of corrosion. The inhibition function of this compound is due to its adsorption on the stainless steel surface and the blocking of the active site. Moreover, it is observed that the presence of various concentrations of this inhibitor has no remarkable effect on the values of corrosion potential, E_{corr}, indicating that this inhibitor is a mixed-type inhibitor. The values of β_c and β_a ($\beta_c \approx 791$ and $\beta_a \approx 707$ mV decade^{-1}) remain almost unchanged with the variation of HDPB concentration. Such behavior demonstrates that the presence of HDPB in the solution has no effect on the mechanism of the dissolution process of the samples, but the adsorbed surfactant molecules mechanically screen the coated part of the electrode and, therefore, protect it from the action of the corrosion medium. The inhibition efficiency, $\eta\%$, of HDPB for the corrosion of SS 304L, SS 316H and SS 304H samples in 0.50 M H_2SO_4 and at 25 °C was calculated using Eq. (1) and the calculated values are listed in Table 2:

$$\eta\% = 100\left(1 - \frac{j_{corr}}{j^{o}_{corr}}\right) \quad (1)$$

where j^{o}_{corr} and j_{corr} are the corrosion current density values in the absence and presence of HDPB in H_2SO_4 solution, respectively, determined by extrapolation of the cathodic and anodic Tafel lines to the corrosion potential.

As shown in Table 2, the inhibition efficiency increases with an increase in the inhibitor concentration and tends to reach the maximum values near its critical micelle concentration, CMC. The increase in the $\eta\%$ with inhibitor concentration is due to an increase in the degree of surface coverage. At a certain concentration, near its CMC, higher efficiency appears which may correspond to the formation of bimolecular layer at the electrode surface (Elze and Fisher, 1952). Indeed, it was shown that surfactant inhibitors give a maximum inhibiting effect at critical micellar concentrations (Hajjaji et al., 1993). Comparing the values of $\eta\%$ for the three samples at a given concentration demonstrates the following sequence: SS 304H > SS 316H > SS 304L.

Figs. 4–6 depict the influence of temperature (25–75 °C) on the potentiodynamic polarization responses for SS 304L in 0.50 M H_2SO_4 solution in the presence of 10^{-2} M HDPB and for SS 316H and SS 304L, respectively, in 0.50 M H_2SO_4 solution in the presence of 10^{-4} M HDPB. The results denote that both cathodic and anodic potentials decrease with an increase of temperature. In addition, increasing the temperature shows that the inhibitor has prevalent effect on the cathodic polarization with respect to the anodic one. The elec-

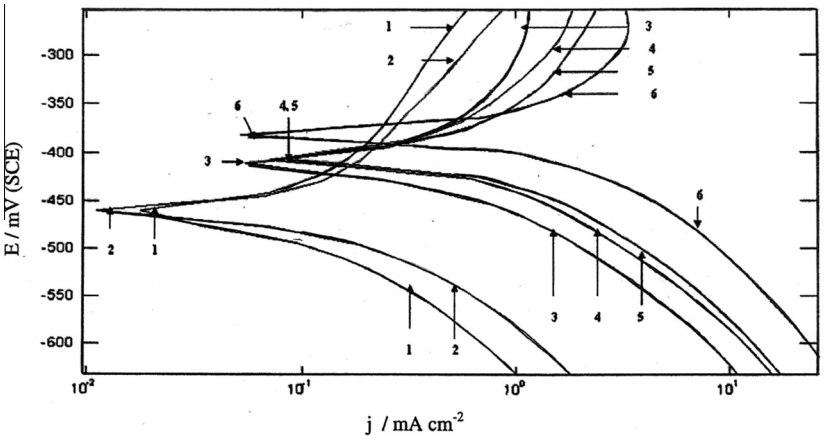

Figure 4 Cathodic and anodic potentiodynamic polarization curves of SS 304L alloy in 0.5 M H_2SO_4 + 10^{-2} M HDPB solution at a scan rate of 20 mV s^{-1} and at different temperatures: (1) 25 °C; (2) 35 °C; (3) 45 °C; (4) 55 °C; (5) 65 °C; (6) 75 °C.

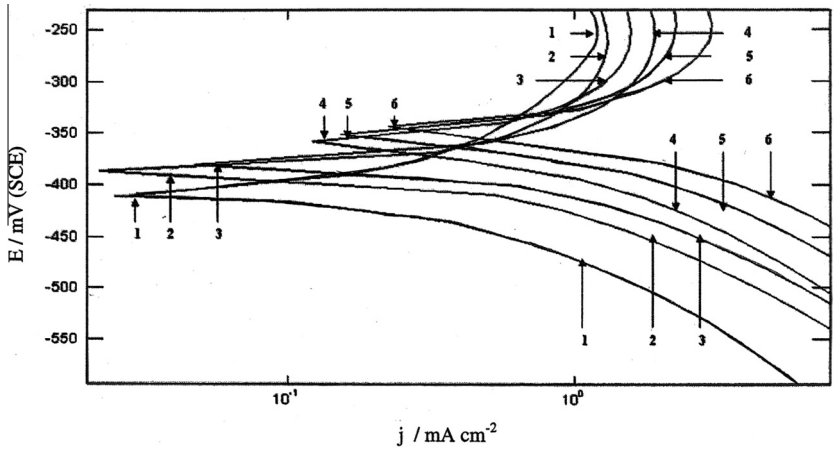

Figure 5 Cathodic and anodic potentiodynamic polarization curves of SS 316H alloy in 0.5 M H_2SO_4 + 10^{-4} M HDPB at a scan rate of 20 mV s^{-1} and at different temperatures: (1) 25 °C; (2) 35 °C; (3) 45 °C; (4) 55 °C; (5) 65 °C; (6) 75 °C.

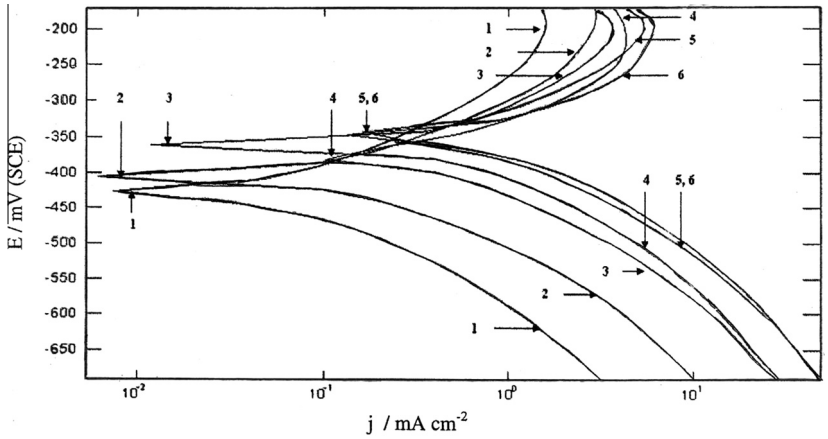

Figure 6 Cathodic and anodic potentiodynamic polarization curves of SS 304H in 0.5 M H_2SO_4 + 10^{-4} M HDPB at a scan rate of 20 mV s^{-1} and at different temperatures: (1) 25 °C; (2) 35 °C; (3) 45 °C; (4) 55 °C; (5) 65 °C; (6) 75 °C.

Table 3 Electrochemical parameters, E_{corr}, j_{corr} and η% obtained from polarization measurements for SS 304L, SS 316H and SS 304H in 0.50 M H_2SO_4 solution (blank) in the absence and presence of HDPB at different temperatures.

Temperature (°C)	SS 304L				SS 316H				SS 304H			
	Blank		Blank + 10^{-2} M HDPB		Blank		Blank + 10^{-4} M HDPB		Blank		Blank + 10^{-4} M HDPB	
	j_{corr} (mA cm^{-2})	j_{corr} (mA cm^{-2})	$-E_{corr}$ (mV)	η%	j_{corr} (mA cm^{-2})	j_{corr} (mA cm^{-2})	$-E_{corr}$ (mV)	η%	j_{corr} (mA cm^{-2})	j_{corr} (mA cm^{-2})	$-E_{corr}$ (mV)	η%
25	22.3	13.0	465	41.9	65.6	29.9	413	54.3	53.5	20.8	445	61.1
35	22.3	14.8	460	33.5	76.5	36.1	395	52.8	64.3	32.7	410	49.2
45	22.6	17.4	412	23.4	78.1	38.3	382	51.0	65.0	41.6	360	36.0
55	24.6	19.5	408	20.6	80.6	39.8	375	50.7	67.0	50.6	355	24.5
65	32.0	25.7	408	19.1	112.5	60.0	360	46.6	70.9	54.3	350	23.3
75	34.1	27.6	380	19.0	113.9	63.2	355	44.5	71.2	56.4	350	20.7

trochemical parameters, E_{corr} and j_{corr} were calculated from Tafel plots and the results are given in Table 3. Inspection of the data reveals that an increase of temperature shifts the values of E_{corr} to more positive potentials. On the other hand, the values of j_{corr} increase with the increasing temperature as a result of the higher dissolution of the three samples at higher temperatures. It is clear that the inhibition efficiency decreases with an increase in temperature, indicating that the adsorption of the inhibitor on the alloy surface belongs to physical adsorption (Table 3).

The thermodynamic functions for the dissolution of the different SS samples in 0.5 M H_2SO_4 in the absence and presence of various concentrations of HDPB were obtained by applying the Arrhenius equation (2) and transition state equation (3), respectively, after replacing the rate of reaction in Arrhenius and transition state equations by j_{corr} in the present study:

$$\log(j_{corr}) = (-E_a^o/2.303RT) + A \quad (2)$$

$$j_{corr} = RT/Nh \exp(\Delta S_a^\circ/R) \exp(\Delta H_a^\circ/RT) \quad (3)$$

where E_a^o is the apparent activation energy, R is the universal gas constant, A is the Arrhenius pre-exponential factor, ΔS_a° is the change in entropy of activation, ΔH_a° is the change in enthalpy of activation, h is Planck's constant and N is the Avogadro's number.

According to Eq. (2) the apparent activation energy E_a^o can be obtained by plotting $\log(j_{corr})$ against $1/T$ as shown in Fig. 7. However, a plot of $\log(j_{corr}/T)$ against $1/T$ according to Eq. (3) should give a straight line with a slope of $(-\Delta H_a^\circ/2.303R)$ and an intercept of $(\log R/Nh - \Delta S_a^\circ/2.303R)$ as shown in Fig. 8. The activation energy E_a^o in the case of SS 304L was found to be 8.8 kJ mol^{-1}, in the absence and 13.6 kJ mol^{-1}, in the presence of HDPB. For SS 316H, it was 11 kJ mol^{-1}, in the absence and 14.7 kJ mol^{-1} in the presence of HDPB. Finally, in the case of SS 304H, it was 6.8 kJ mol^{-1} in the absence and 18.8 kJ mol^{-1} in the presence of HDPB. These results mean that the addition of HDPB to the acid solution increases E_a^o and the extent of the increase is proportional to the inhibitor concentration, indicating that the energy barrier for the corrosion reaction increases with HDPB concentration. In other words, the corrosion reaction will be further pushed to the surface sites that are characterized by progressively higher values of E_a^o as the concentration of the inhibitor in the acid solution becomes larger.

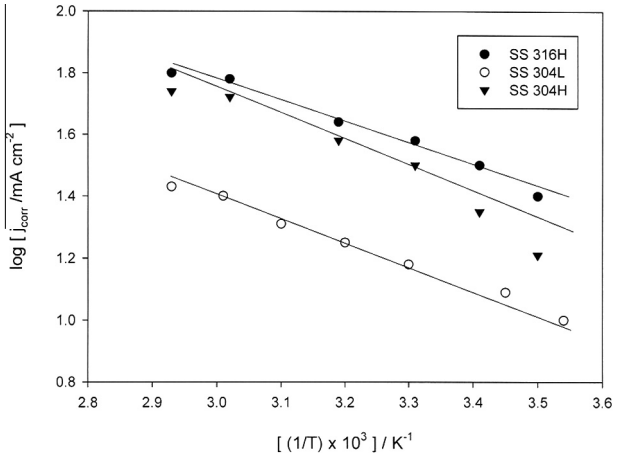

Figure 7 Arrhenius plots of $\log(j_{corr})$ vs. $(1/T)$ for SS 304L alloy in 0.50 M H_2SO_4 + 10^{-2} M HDPB solution and for SS 316H and SS 304H alloys in 0.50 M H_2SO_4 + 10^{-4} M HDPB solution.

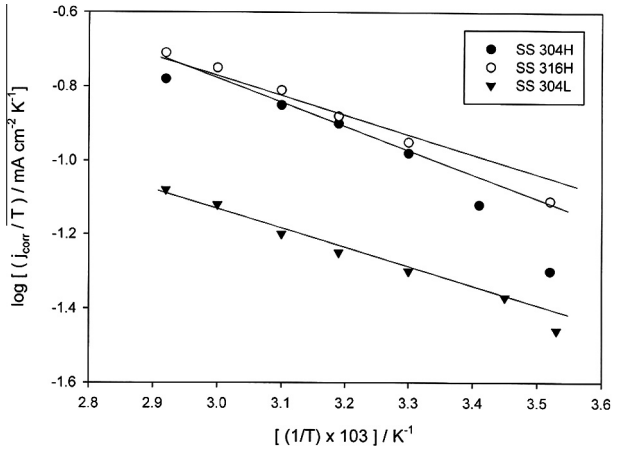

Figure 8 Transition state plots of $\log(j_{corr}/T)$ vs. $(1/T)$ for SS 304L alloy, in 0.50 M H_2SO_4 + 10^{-2} M HDPB solution and for SS 316H and SS 304H alloys in 0.50 M H_2SO_4 + 10^{-4} M HDPB solution.

The entropy of activation ΔS_a° in the absence and presence of HDPB is large and negative (Table 4). This implies that the activated complex in the rate determining step represents an association rather than a dissociation step, meaning that a decrease in disordering takes place on going from reactants to the activated complex (Frignani et al., 1983; Bentiss et al., 2001).

In systems where temperature increases result in lower protection efficiency, a negative ΔH_{ads} is expected. This means, weaker surface interactions at high temperatures. Finally, the magnitude of the difference between the enthalpy or entropy of activation in the presence and absence of inhibitor is a measure of its degree of inhibition. A higher difference means better inhibition and vice versa. In the present study, the physisorption is evident from the decrease in inhibition efficiency with temperature; the apparent activation energy of the corrosion is higher in the presence of HDPB than in its absence and the low positive value of ΔH_{ads}.

3.2. Electrochemical impedance measurements

In order to gain more information about the corrosion inhibition phenomena, electrochemical impedance spectroscopy (EIS) measurements were carried out for the three stainless steel samples in 0.50 M H_2SO_4 solution. Figs. 9–11 show the EIS spectra; Nyquist complex planes and Bode phase angle diagrams for SS 304L, SS 316H and SS 304H samples, respectively, in aerated 0.50 M H_2SO_4 with and without various concentrations of HDPB at 25 °C and at OCP as a function of frequency (30 kHz to 1 Hz). The equivalent circuit models used to fit the experimental results are given in Fig. 12 as previously reported (Al Sayed, 1996; Sekine et al., 1992). Charge–transfer resistance (R_{ct}), double layer capacitance (C_{dl}) and the charge transfer kinetics of SS alloys were determined using EIS-measurements and the data are listed in Table 5. The equivalent circuit model in Fig. 12(a) can be given in a simplified equivalent circuit model as in Fig. 12(b). The measured complex-plane impedance plot is similar to that calculated by the equivalent circuit model. It is worth noting that in case of SS 304L, the low concentration (10^{-6}–10^{-3} M) of HDPB gives low values of R_{ct} (lower than that of the blank) and high values of the C_{dl} (higher than that of the blank) indicating acceleration of corrosion. However, higher concentrations of HDPB leads to an increase in the value of R_{ct} and a decrease in the value of C_{dl}. The decrease in C_{dl} values with HDPB concentration indicates as increase in the surface coverage of the inhibitor. These results agree well with the data obtained by potentiodynamic polarization measurements. On the other

Table 4 Thermodynamic activation functions ΔH_a° and ΔS_a° for the corrosion process associated with polarization measurements recorded for SS 304L, SS 316H and SS 304H in 0.50 M H_2SO_4 solution (blank) in the absence and presence of HDPB, obtained by applying transition state equation.

SS 304L				SS 316H				SS 304H			
ΔH_a° (kJ/mol)		$-\Delta S_a^\circ$ (J/mol K)		ΔH_a° (kJ/mol)		$-\Delta S_a^\circ$ (J/mol K)		ΔH_a° (kJ/mol)		$-\Delta S_a^\circ$ (J/mol K)	
Blank	Blank + 10^{-2} M HDPB	Blank	Blank + 10^{-2} M HDPB	Blank	Blank + 10^{-4} M HDPB	Blank	Blank + 10^{-4} M HDPB	Blank	Blank + 10^{-4} M HDPB	Blank	Blank + 10^{-4} M HDPB
6.1	11.1	246	234	9.4	12.2	226	230	4.2	16.9	245	216

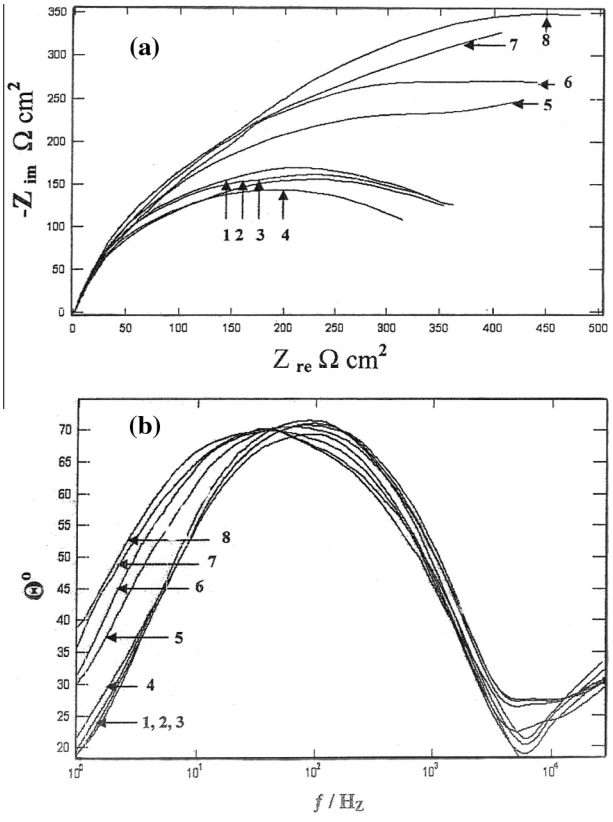

Figure 9 AC impedance; Nyquist (a) and Bode (b) diagrams recorded for SS 304L alloy in 0.50 M H_2SO_4 solution in the absence and presence of various concentrations of HDPB at the respective open circuit potentials at 25 °C. (1) Blank; (2)10^{-6} M; (3) 10^{-5} M; (4) 10^{-4} M; (5) 10^{-2} M; (6) 0.02 M; (7) 0.03 M; (8) 0.04 M HDPB.

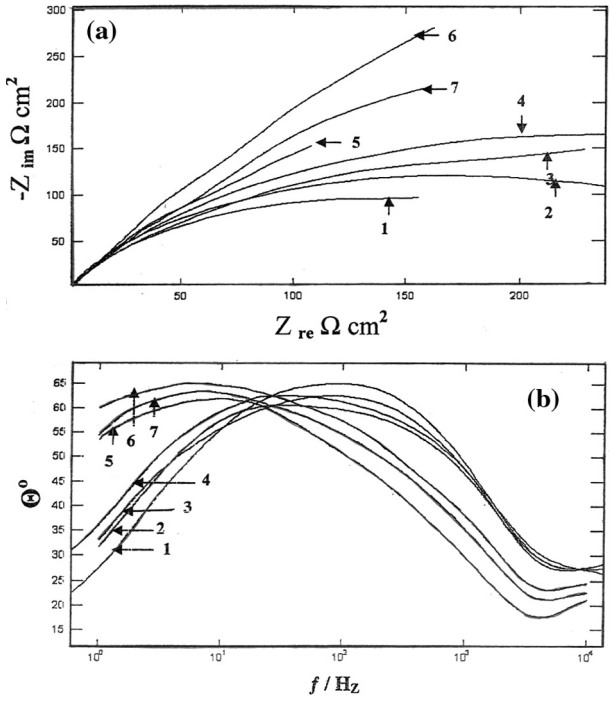

Figure 10 AC impedance; Nyquist (a) and Bode (b) diagrams recorded for SS 316H alloy in 0.50 M H_2SO_4 solution in the absence and presence of various concentrations of HDPB at the respective open circuit potentials at 25 °C. (1) Blank; (2) 10^{-6} M; (3) 10^{-5} M; (4) 10^{-4} M; (5) 10^{-3} M; (6)10^{-2} M; (7) 0.02 M HDPB.

hand, it is observed that in the case of samples SS 316H and SS 304H, the values of R_{ct} increase while those of C_{dl} decrease with increasing the inhibitor concentration in all the solutions studied. The addition of HDPB to the solution does not alter the profile of AC impedance displaying similar mechanisms for corrosion of these samples in the uninhibited and inhibited solutions. The capacitance loop of Nyquist plot is a depressed semicircle in all cases. The increasing compactness of the film is confirmed by the Nyquist plots. They always present a semicircle, which is more depressed with increasing the concentrations of the inhibitor. According to the literature this is attributed to the formation of a film of increasing compactness (Schiller and Strunz, 2001).

The inhibition efficiency, $\eta\%$, calculated from the EIS measurements was given by the following equation:

$$\eta\% = 100\left(\frac{R_{ct} - R_{ct}^{o}}{R_{ct}}\right) \quad (4)$$

where R_{ct}^{o} and R_{ct} are the charge–transfer resistances for uninhibited and inhibited solutions, respectively.

It is found that $\eta\%$ enhances with inhibitor concentration and tends to reach a maximum at CMC of HDPB (Table 5). It is clear that the values of $\eta\%$ determined by the two different methods are comparable and agree well.

The effect of immersion time (0–120 min) on the performance of HDPB inhibitor on the corrosion behavior of the three samples was investigated in 0.50 M H_2SO_4 containing

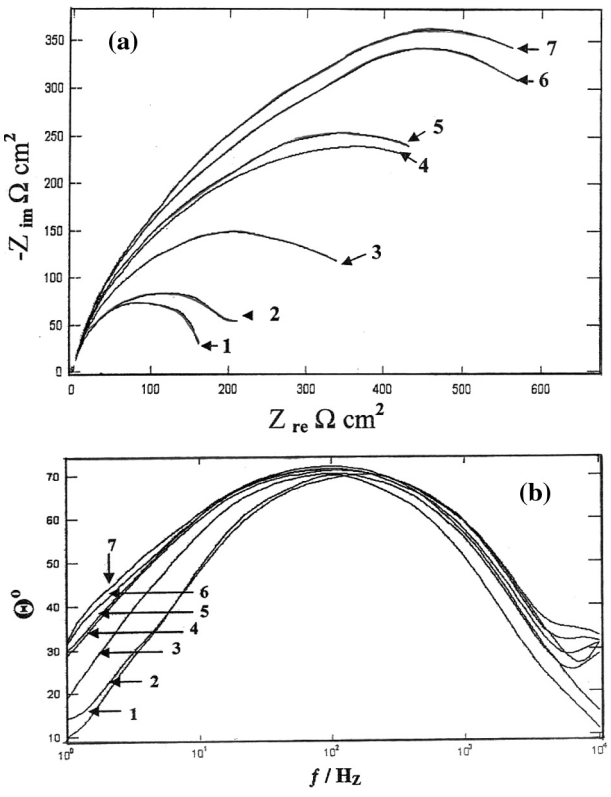

Figure 11 AC impedance; Nyquist (a) and Bode (b) diagrams recorded for SS 304H alloy in 0.50 M H_2SO_4 solution in the absence and presence of various concentrations of HDPB at the respective open circuit potentials at 25 °C. (1) Blank; (2) 10^{-6} M; (3) 10^{-5} M; (4) 10^{-4} M; (5) 10^{-3} M; (6) 10^{-2} M; (7) 0.02 M HDPB.

10^{-2} M HDPB for the SS 304L and 10^{-4} M HDPB for SS 316H and SS 304H at 25 °C by AC impedance at OCP (Table 6). The impedance parameters R_{ct}, C_{dl} and $\eta\%$ were determined at various time intervals for the three stainless steel samples. The dependence of $\eta\%$ on the immersion time is shown in Table 6. It is clear that at first, the inhibition efficiency increases with immersion time up to a certain critical time, which depends on the composition of the sample. Beyond this critical time, it deteriorates. The increase in the inhibition is due to an

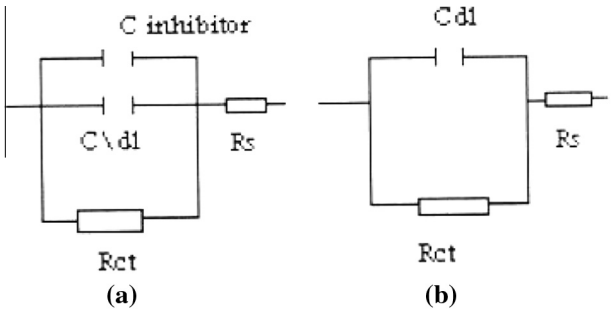

Figure 12 Equivalent electronic circuit model (a) can be given in a simplified equivalent circuit model (b), R_s and R_{ct} are the solution and charge transfer resistance, respectively. $C_{inhibitor}$ is the capacitance of parts that the inhibitor is adsorbed. C'_{dl} is the capacitance of parts that the inhibitor is not adsorbed and C_{dl} is the apparent double layer capacitance.

increase in the surface coverage. The deterioration in $\eta\%$ can be correlated to an increase in corrosion products in the solution (Horvath et al., 1994) and also to increase in the real surface area by time (Singh and Gaur, 1995).

3.3. Adsorption isotherm

In order to get more knowledge about the mode of adsorption of HDPB on the surface of the three SS samples, the data obtained from the potentiodynamic polarization and AC impedance techniques have been tested with the well known adsorption isotherms. Temkin isotherm (Eq. (5)) was found to fit well the experimental data

$$a\theta = \ln KC \tag{5}$$

where θ is the degree of surface coverage by HDPB molecules ($\theta = \eta/100$), a is the molecular interaction parameter, which depends on the lateral interaction force among the adsorbed inhibitor molecules on the surface and on the degree of heterogeneity of the stainless steel sample, C is the concentration of HDPB in the solution and K is the equilibrium constant for adsorption process of the inhibitor. It was found that the plot of θ against C shown in Fig. 13 using polarization as well as impedance techniques obeys Temkin adsorption isotherms for adsorption of the HDPB at 25 °C on the surfaces of SS 304L, SS 316H and SS 304H in 0.50 M H_2SO_4. The calculated

Table 5 AC impedance data R_{ct}, C_{dl} and $\eta\%$ recorded for SS 304L, SS 316H and SS 304H in 0.50 M H_2SO_4 solution in the absence and presence of various concentrations of HDPB, at 25 °C.

Conc. (M)	SS 304L			Conc. (M)	SS 316H			Conc. (M)	SS 304H		
	R_{ct} (Ω cm^2)	C_{dl} (μF cm^{-2})	$\eta\%$		R_{ct} (Ω cm^2)	C_{dl} (μF cm^{-2})	$\eta\%$		R_{ct} (Ω cm^2)	C_{dl} (μF cm^{-2})	$\eta\%$
0.000	436.3	172.6		0.000	266.7	676.3		0.00	173.8	266.0	
10^{-6}	365.3	246.0		10^{-6}	355.0	650.0	24.9	10^{-6}	313.3	260.0	44.5
10^{-5}	407.5	238.0		10^{-5}	578.0	611.0	53.9	10^{-5}	406.7	252.0	57.3
10^{-4}	423.3	236.7		10^{-4}	588.5	610.0	54.7	10^{-4}	449.2	249.0	61.1
10^{-3}	613.7	235.6	28.9	10^{-3}	693.9	596.0	61.8	10^{-3}	648.3	247.0	73.2
10^{-2}	713.8	234.0	38.9	10^{-2}	1525	475.0	82.5	10^{-2}	1000	222.0	82.6
0.02	1265	212.0	65.6	0.02	1439	497.0	81.5	0.02	1097	217.0	84.7
0.03	1458	206.0	70.1								

Table 6 Charge transfer resistance R_{ct} and double layer capacitance C_{dl} associated with EIS measurements recorded for SS 304L, SS 316H and SS 304H at different immersion times and at 25 °C, in 0.50 M H_2SO_4 solution (blank) in the absence and presence of HDPB.

Immersion time (min)	SS 304L			SS 316H			Immersion time (min)	SS 304H		
	Blank + 10^{-2} M HCPB			Blank + 10^{-4} M HCPB				Blank + 10^{-4} M HCPB		
	R_{ct} (Ω cm^2)	C_{dl} (μF cm^{-2})	η%	R_{ct} (Ω cm^2)	C_{dl} (μF cm^{-2})	η%		R_{ct} (Ω cm^2)	C_{dl} (μF cm^{-2})	η%
Blank	436.3	172.6		266.7	676.3		Blank	173.8	266.0	
0.00	713.8	234.0	38.9	588.5	610.0	54.7	0.00	449.2	249.0	61.3
5.00	909.4	215.0	52.0	639.3	590.0	58.3	5.00	988.8	178.0	82.4
15.0	1071.0	185.0	59.3	715.8	544.0	62.7	10.0	1111	162.0	84.4
30.0	1154.0	179.0	62.2	724.5	490.0	63.2	15.0	926.5	182.0	81.2
60.0	1215.0	165.0	64.1	1866	422.0	85.7	30.0	498.3	279.0	65.1
120	1073.0	183.0	59.3	1432	430.0	81.4	60.0	540.4	275.0	67.8
							120	626.2	235.0	72.3

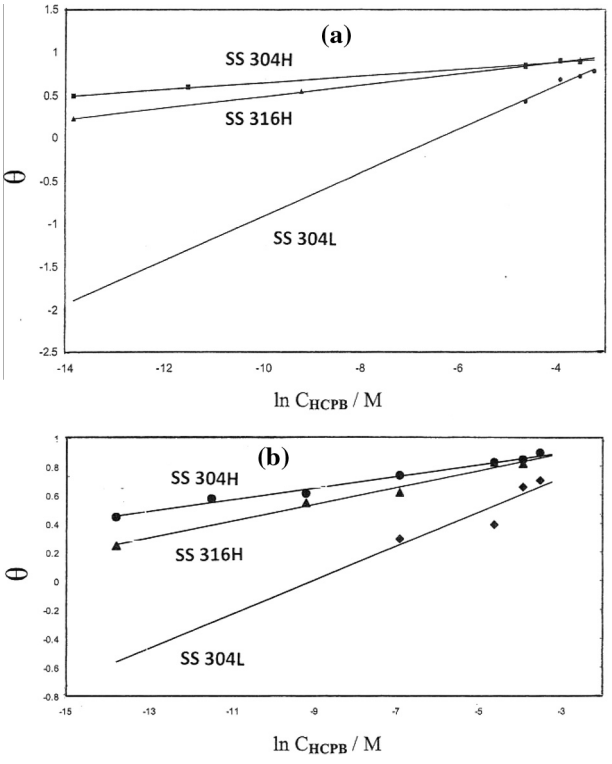

Figure 13 Curve fitting of (a) potentiodynamic polarization and (b) impedance data obtained for the three alloys in 0.50 M H_2SO_4 solution containing various concentrations of HDPB to Temkin adsorption isotherm at 25 °C.

values of the interaction parameter a, the adsorption equilibrium constant K, and the free energy of adsorption ΔG°_{ads} at different HDPB concentrations using Temkin isotherm for the three alloys are given in Table 7.

The equilibrium constant K is related to the free energy of adsorption, ΔG°_{ads}, by the following equation (Do, 1998):

$$K = (1/55.5)\exp(-\Delta G^{\circ}_{ads}/RT) \quad (6)$$

where R is the universal gas constant and T is the absolute temperature. It is clear that the value of the lateral interaction parameter a increases from alloy SS 304L to SS 304H. The calculated values of ΔG°_{ads} are low and negative suggesting that the nature of the inhibitor adsorption is mainly physisorption and spontaneous. The negative values of ΔG°_{ads} as well as the values of K increase from sample SS 304L to sample SS 304H.

In general, the adsorption processes of the organic inhibitor are affected by several factors, such as; the nature of the metal surface, the chemical structure of the inhibitor, the distribution of the charge in the molecule, the type of aggressive electrolyte and the type of interaction between the inhibitor molecule and the metallic surface (Zucchi et al., 1992; Bockris and Yang, 1991; Kertit et al., 1989).

On the other hand, the addition of HDPB will introduce Br^- anions to the sulfuric acid solution. Br^- anions will be the first adsorbed at the electrode/solutions interface through electrostatic attraction and create an excess negative charge toward the solution phase and favor more adsorption of positively charged quaternary ammonium cations. Thus, the quaternary ammonium cation will be electrostatically adsorbed on the electrode surface covered with primarily adsorbed bromide anions. In addition, the adsorption of HDPB molecules on the stainless steel surface may take place through the donor–acceptor links between the π-electrons of

Table 7 Inhibitor binding constant K, free energy of binding ΔG°_{ads} and molecular interaction parameter a recorded for SS 304L, SS 316H and SS 304H at 25 °C obtained by applying Temkin adsorption isotherm on potentiodynamic polarization and EIS data.

Sample	K		ΔG°_{ads} (kJ/mol)		a	
	Polarization	Impedance	Polarization	Impedance	Polarization	Impedance
SS 304L	585	402	−25.3	−24.8	4.0	3.4
SS 316H	35,872,454	73,250,945	−52.2	−54.8	15.1	17.1
SS 304H	3.9×10^{11}	9.48×10^{10}	−74.8	−72.6	25.9	25.3

the pyridinium ring and the empty d-orbital of the Fe atom of the stainless steel.

The adsorption of HDPB at the electrode solution surface cannot be simply considered as an electrostatic adsorption attributed to the synergistic effect of Br^- ions, the adsorption of the hydrocarbon chain on the electrode surface must be considered at the same time. Compared with SDS ($C_{12}H_{25}SO_4^-$) ions, the head of HDPB is larger and the hydrocarbon chain is longer. This may explain why the η% of HDPB is much higher than that of SDS for the corrosion of the three stainless steel samples in 0.50 M H_2SO_4 (Ibrahim et al., unpublished data).

4. Conclusions

(i) HDPB behaves as an inhibitor for the corrosion of the Egyptian austenitic stainless steels SS 304L, SS 316H and SS 304H in 0.5 M H_2SO_4 solution.
(ii) HDPB molecule is found to affect both the anodic and cathodic processes by simple blocking of the active sites of the metal, i.e. HDPB is a mixed inhibitor.
(iii) The inhibition efficiency increases with increasing inhibitor concentrations while decreases with increasing temperature.
(iv) The results of electrochemical impedance spectroscopy techniques and Tafel polarization measurements are in good agreement.
(v) The inhibition is due to the adsorption of the inhibitor molecules on the samples and the blocking of active sites.
(vi) The adsorption of HDPB inhibitor on the stainless steel surfaces in 0.5 M H_2SO_4 solution obeys a Temkin adsorption isotherm.
(vii) Activation-free energies, enthalpies, and entropies for the inhibition process of HDPB were determined.

References

Abd El Maksoud, S.A., 2004. J. Electroanal. Chem. 565, 321.
Abd El Rehim, S.S., Abd El Haleem, S.M., Shalaby, M.Sh., 1985. Surf. Technol. 26, 77.
Abd El Rehim, S.S., Amin, M.A., Moussa, S.O., Ellithy, A.S., 2008. Mater. Chem. Phys. 112, 898.
Al Sayed, A., 1996. Corros. Prevent. Control 43, 29.
Ameer, M.A., Fekry, A.M., El-Taib Heakal, F., 2004. Electrochim. Acta 50, 43.
Bentiss, F., Traisnel, M., Lagrenee, M., 2001. J. Appl. Electrochem. 31, 41.
Bockris, J.O.M., Yang, B., 1991. J. Electrochem. Soc. 138, 2237.
Do, D., 1998. Adsorption Analysis: Equilibria and Kinetics. Imperial College Press, pp. 10–60.
Elze, J., Fisher, H., 1952. J. Electrochem. Soc. 99, 259.
Frignani, A., Zucchi, F., Monticelli, C., 1983. Br. Corros. J. 18, 19.
Hajjaji, N., Ricco, I., Srhiri, A., 1993. Corros. Sci. 49, 326.
Horvath, T., Kalman, E., Kuston, G., Rauscher, A., 1994. Br. Corros. J. 29, 215.
Ibrahim, M.A.M., 2000a. J. Chem. Technol. Biotechnol. 75, 745.
Ibrahim, M.A.M., 2000b. Plat. Surf. Finish. 87, 67.
Ibrahim, M.A.M., Korablov, S.F., Yoshimura, M., 2002. Corros. Sci. 44, 815.
Ibrahim, M.A.M., Amin, M.A., Abbass, M.A., 2004. Trans. Inst. Met. Finish. 82, 87.
Ibrahim, M.A.M., Abd El Rehim, S.S., El Nagger, M.M., Abbass, M.A., 2006. J. Appl. Surf. Finish. 1, 227.
Ibrahim, M.A.M., Rehim, Abd.El., Mossad, M.M., 2008. Mater. Chem. Phys. 115, 80.
Ibrahim, M.A.M., Abd El Rehim, S.S., Hamza, M.M., unpublished data.
Kertit, S., Elkhely, A., Aride, J., Srhiri, A., Ben-Bachir, A., Etman, M., 1989. J. Appl. Electrochem. 19, 83.
Larabi, L., Harek, Y., Traisnel, M., Mansri, M., 2004. J. Appl. Electrochem. 34, 833.
Podobaev, N.I., Stolyarov, A.A., 1971. Prot. of Metals 7, 68.
Popova, A., Sokolova, E., Raicheva, S., Christov, M., 2003. Corros. Sci. 45, 33.
Riggs, O.L., 1973. Corrosion Inhibitors. NACE Houston, TX.
Rybalka, K.V., Beketaeva, L.A., Davydov, A.D., 2006. Russ. J. Electrochem. 42 (4), 370.
Saleh, M.M., 2006. Mater. Chem. Phys. 98, 83.
Schiller, C.A., Strunz, W., 2001. Electrochim. Acta 46, 3619.
Schweinsberg, D.P., Ashworth, V., 1988. Corros. Sci. 28, 539.
Sekine, I., Sabongi, M., Hagiuda, H., Oshike, T., Yuasa, M., Imahama, T., Shibata, Y., Wake, T., 1992. J. Electrochem. Soc. 139, 3167.
Singh, D.N.N., Gaur, B., 1995. Corrosion 51, 593.
Tavakoli, H., Shahrabi, T., Hosscini, M.G., 2008. Mater. Chem. Phys. 109, 281.
Yang, Q., Luo, J.L., 2001. Electrochim. Acta 46, 851.
Zucchi, F., Trabanelli, G., Brunoro, G., 1992. Corros. Sci. 33, 1135.